An Acoustic Network Navigation System

Andrea Munafò and Gabriele Ferri
NATO STO Centre for Maritime Research and Experimentation, Research Department, Viale San Bartolomeo 400, 19126, La Spezia, Italy
e-mail: andrea.munafo@cmre.nato.int, gabriele.ferri@cmre.nato.int

Received 1 February 2016; accepted 2 February 2017

This work describes a system for acoustic-based navigation that relies on the addition of localization services to underwater networks. The localization capability has been added on top of an existing network, without imposing constraints on its structure/operation. The approach is based on the inclusion of timing information within acoustic messages through which it is possible to know the time of an acoustic transmission in relation to its reception. Exploiting such information at the network application level makes it possible to create an interrogation scheme similar to that of a long baseline. The advantage is that the nodes/autonomous underwater vehicles (AUVs) themselves become the transponders of a network baseline, and hence there is no need for dedicated instrumentation. The paper reports at sea results obtained from the COLLAB–NGAS14 experimental campaign. During the sea trial, the approach was implemented within an operational network in different configurations to support the navigation of the two Centre for Maritime Research and Experimentation Ocean Explorer (CMRE OEX) vehicles. The obtained results demonstrate that it is possible to support AUV navigation without constraining the network design and with a minimum communication overhead. Alternative solutions (e.g., synchronized clocks or two-way-travel-time interrogations) might provide higher precision or accuracy, but they come at the cost of impacting on the network design and/or on the interrogation strategies. Results are discussed, and the performance achieved at sea demonstrates the viability to use the system in real, large-scale operations involving multiple AUVs. These results represent a step toward location-aware underwater networks that are able to provide node localization as a service. © 2017 Wiley Periodicals, Inc.

1. INTRODUCTION

The rapid attenuation of radio-frequency signals and the unstructured nature of the undersea environment make autonomous underwater vehicles (AUVs) navigation and localization a challenging task (Paull, Saeedi, Seto, & Li, 2014a). Underwater vehicles are unable to rely on the Global Positioning System (GPS) to navigate during their missions, and the absence of some sort of an external reference implies that they have to base their navigation only on their own proprioceptive information (dead reckoning), as obtained from Doppler Velocity Loggers (DVL), Inertial Navigation Systems (INS), etc. However, regardless of the quality of the sensors used, the error in the position estimate based on dead reckoning grows without bound. The growth in the navigation error goes from around $\sim 0.1\%$ of the distance traveled for AUVs operating in shallow water, where the DVL can obtain a bottom lock, to as much as 20% of error for vehicles with low-cost inertial systems. In such cases, traditional methods for bounding the navigation error require the vehicle to periodically surface to get a GPS fix, or the deployment of static beacons [long baseline (LBL)] to help the localization of the AUVs. The downsides of these approaches are evident. In the first case, the vehicle has to interrupt its main task to obtain a position fix on surface, hence reducing its effectiveness. Also, this is an operation that takes more time the deeper the vehicle has to work at. The deployment of fixed beacons increases the working flexibility of the vehicles during the mission providing a fixed reference, but it requires a great deal of instrumentation to be deployed and calibrated at each site. This limits the operational area to a few square kilometers, posing constraints on the freedom of movement of the vehicles. Depending on the scenario, this might be incompatible with the higher level mission requirements (e.g., operation in denied areas). This work moves in a different direction and aims at exploiting the presence of underwater acoustic networks to provide supporting infrastructures for the navigation of autonomous vehicles. The envisioned scenario is that of a persistent autonomous underwater sensor network with a navigational layer that enables location-aware services without constraining network protocols/structure. This layer makes it possible for the nodes/AUVs that join the communication infrastructure to receive localization data.

The development of mobile underwater sensor networks has been boosted by the progress in acoustic modems.

Direct correspondence to: Andrea Munafò, e-mail: andrea.munafo@cmre.nato.int

 © 2017 Wiley Periodicals, Inc.
View this article online at wileyonlinelibrary.com • DOI: 10.1002/rob.21714

Acoustic communication devices are in fact becoming more and more network conscious and able to provide a number of services that can be exploited at higher network levels (Akyildiz, Pompili, & Melodia, 2005; Pompili & Akyildiz, 2010). To provide network localization, this work exploits one of such services, as made available from the physical layer (i.e., acoustic modems) to the upper layers of the network (Kebkal, Kebkal, Kebkal, & Petroccia, 2014): the availability of precise transmission and reception timing. Encoding such information in the acoustic packet makes it possible to calculate the round-trip-time (rtt) of the message exchange at application level. This information is then used, together with the node's positions (that can be encoded in different packets) and the sound velocity profile to calculate the range from the receiver to the transmitter. The underwater sensor network becomes able to create an LBL-like Hunt et al. (1974) interrogation scheme simply based on the knowledge of the exact time of an acoustic transmission in relation to its time of reception. This provides a way to use modems to implement an interrogation scheme for AUV positioning without the need to have synchronized clocks or dedicated instrumentation. Such a system would be exploitable not only for cheaper vehicles that cannot rely on expensive navigation systems, but also for more capable vehicles to enhance their persistence in the field and to extend their operational usage, for example, to situations where the DVL bottom tracking—one of the traditional ways of limiting the navigation error—is not possible. Note also that the availability of navigational services at network level increases the overall system flexibility, making it possible to tune the localization needs to the requirements of the mission (e.g., more localization packets might be sent when the vehicle position uncertainty is higher). Work on including localization data into acoustic communications has seen, in recent years, a significant effort. Examples of such effort can be found in Freitag, Johnson, Grund, Singh, & Preisig (2001); Freitag et al. (2005); Singh et al. (2006), and Hiller, Steingrimsson, and Melvin (2012), where some of the leading manufacturers of acoustic modems focus on making the acoustic modem itself able to produce localization data. The work presented in this paper aims at generalizing these methods, realizing a navigational layer in the ad hoc network protocol, which is able to provide navigational and localization services to all the nodes of the network. This permits the acoustic network to have heterogeneous capability (when a node joins the network it can also receive localization data, together with normal network traffic), and applicability to a range of modems, and to be explicitly tailored to software-defined modems (Chitre, Bhatnagar, & Soh, 2014; Potter et al., 2014).

In this paper, we report the implemented solutions and the performance of an acoustic network navigation system measured in the field. More in details we discuss (1) the impact of the addition of localization data within an operational network that comes with its own constraints and that cannot be used only for vehicle localization purposes; (2) the accuracy and precision of the range measurements obtained using the proposed interrogation scheme within the network constraints; (3) the capability of the acoustic network navigation system to provide navigational services that can be used by AUVs to limit their navigation error and hence to increase their operational abilities. Understanding these factors is of paramount importance for the deployment of an effective and robust system. The underlying philosophy is to build a navigational layer on the top of existing network solutions without requiring specific constraints to the network itself or ad hoc means (e.g., synchronized clocks or physical level acknowledgements) and to report the obtained performance. We believe that reporting field performance is of value in itself since it may orient applications and research toward refinements or different choices, with the long-term objective of achieving operational implementations of location aware underwater networks. The localization scheme has been tested within a fully operational antisubmarine acoustic network, with typical distances between the nodes from 2 to 10 km. Mission requirements for the operation of this specific network requires that the addition of navigational data must not interfere with the normal traffic; hence, the communication overhead required for the localization must be kept at a minimum. From an experimental perspective, the first contribution of this work is the presentation of the results obtained within the activities of the COLLAB–NGAS14 experimental campaign. During the experiment, a six-node network was deployed in 60 m of water. The network was composed of two OEX AUVs, two wave gliders, one fixed gateway buoy, and the NRV Alliance, equipped with a modem over the side. The experiment demonstrated how the availability of navigational services within the acoustic network was key to support the navigation of AUVs while they were executing autonomous missions (Ferri, Munafò, Goldhahn, & LePage, 2014), and thus key in increasing their operative abilities. The COLLAB–NGAS14 part, devoted to testing AUV navigation, was executed from October 29 to October 31, 2014, off the coast of Tuscany, Italy. The second experimental contribution is to provide a quantitative comparison of the navigation performance with varying number of network nodes and localization packets. This second part of the work has been done in postanalysis reducing the number of localization data collected during the experimental campaign, and varying the number of nodes participating in the measurements. Results show how the inclusion of localization data to the normal network traffic can be instrumental in enhancing the AUVs' navigation, even at long ranges and with sporadic communication. The presented results represent a step toward the usage of AUVs in deep waters, where DVL bottom lock cannot be established, or whenever more traditional approaches show their limits. This also opens up a wide set of scenarios where teams of AUVs, possibly equipped with quite limited or cheap sensors, can rely on a network infrastructure to achieve better navigation and therefore mission performance.

The reminder of this paper is organized as follows: Section 2 describes previous work in the area of acoustic-based navigation. Section 3 describes how it is possible to add localization services to networked acoustic communications. Section 4 reports the mathematical framework for the Extended Kalman Filter (EKF) used to incorporate the network range measurements. Section 5 describes and reports results from the COLLAB–NGAS14 experimental campaign. Finally, Section 6 draws some conclusions.

2. PREVIOUS WORK

The problem of bounding the navigation error of AUVs has been approached from several perspectives. Probably the most common approach used in in-the-field underwater operations is that of relying on acoustic-based positioning systems, such as long baseline (LBL), short baseline (SBL) and ultra short baseline (USBL). Most of these systems are based on the computation of the ranges and/or the bearings between a set of acoustic sensors, with known positions, and a target that must be localized. This is done by measuring the times of arrival (TOA) or the time differences of arrival (TDOA) of the acoustic signals that arrive at an array of sensors (Paull et al., 2014a). The main component of an LBL system is a set of transponders that are deployed onto the sea floor in an array (Hunt et al., 1974). These transponders that can be spaced by several kilometers represent the baseline. In a typical application, the target to be localized sequentially interrogates each transponder and receives a reply. Measuring the round trip time, the interrogator is hence able to calculate the range and to calculate its position using trilateration. LBL systems are used for wide area and long-range navigation. Its precision depends on a number of factors: target depth, size of the baseline, frequency of the interrogation, and deployment precision. Overall, the LBL provides accurate control and high repeatability. If there is redundancy, as for example, when the baseline is composed of four or more transponders, the quality of the localization can be improved. LBL operation might be costly and time consuming as it requires the deployment, calibration, and recovering of multiple transponders. In certain scenarios this might be impractical. The area is limited by geometry and communication range, and once it has been setup it cannot be changed without recovering the system and redeploying it.

In the SBL (Milne, 1983; Vickery, 1998), the baseline is realized through units installed on-board a support ship at a distance between 10 and 50 m from each other. The principle of operation is hence similar to that of an LBL. However, the reduced length of the baseline, usually much smaller than the distance from the target to the transponders, makes the accuracy of the SBL lower than that of the LBL (the larger is the baseline, the better is the positioning accuracy). No fixed beacons on the seabed are required, and the system provides position fixes relative to the surface vessel.

An USBL [Vickery (1998); Milne (1983)] consists of a unique device which includes both a transmitter and a receiver (transceiver). The USBL is usually positioned under the hull of a ship, whereas a transponder is installed onboard the target to be localized. The USBL transceiver emits an acoustic wave, which is detected by the transponder. The transponder replies with an acoustic response to the USBL, which, being equipped with a phase transducer array (three or more transducers usually separated from each other by less than 10 cm), is able to resolve both range and bearing to the transponder. The target is hence localized with an accuracy that depends on the installation and calibration of the transceiver aboard the ship, as well as on the accuracy with which the inertial position and attitude of the ship can be determined. USBL systems are simple to operate and have relatively moderate prices. Their position estimates are usually worse than those obtained with LBL or SBL systems and very sensitive to attitude errors on the transceiver.

All the aforementioned methods are based on querying one or more remote transponders, while measuring the two-way-travel-time of the acoustic packet. Alternative approaches have been based on using the One-Way-Travel-Time (OWTT), by relying on time synchronization between the nodes. In this case, accurate one-way travel time ranging can be determined by precisely knowing the times of transmit and receive of an underwater acoustic communications packet (Walls & Eustice, 2011). An example, on the usage of OWTT, can be found in Vaganay, Leonard, Curcio, and Willcox (2004), where the availability of high-precision clocks made it possible to overcome some of the limitations of the LBL. The proposed concept, called Moving Long Baseline (MLBL), is that dedicated vehicles can be fitted with accurate navigation systems and used as moving reference transponders to which other, less capable, vehicles can acoustically range to update their position. By removing the need for preinstalled navigation aids, the MLBL system enlarges the area of operation while simultaneously reducing the operational and logistical requirements. Furthermore, the MLBL concept has been extended by Fallon, Papadopoulos, Leonard, and Patrikalakis (2010) to using only one surface maneuvering vehicle as navigational aid of one or more AUVs providing geo-referenced range measurements. More recently, Webster, Eustice, Singh, and Whitcomb (2012) have shown, in postprocessing, how single-beacon OWTT navigation can be successfully applied for high-precision absolute navigation of underwater vehicles for missions with length scales up to 100 km, without the need for fixed navigation references. This approach easily scales to a multinode environment, as the overall update rate for each vehicle remains constant. When one node interrogates the network, all the listeners can measure the time-of-flight between each of them and the source node. The disadvantage is in an increased complexity (and cost) in the hardware design since all the nodes must have their own synchronized clock.

The above examples show dedicated solutions for distributed localization. However, when a vehicle is part of a team or acts as a mobile node of a network, it is already part of an infrastructure that can be used to help its localization. One example of such an approach has been reported in Rice (2002, 2005), where the Seaweb underwater acoustic network was able to provide acoustic ranging, localization, and navigation functionalities supporting manned and unmanned mobile nodes as members of the network. In this case, the range measurement between a pair of communicating nodes was obtained as a by-product of the handshaking at the modem physical level. The idea of exploiting an existing communication infrastructure is also proposed in Furfaro and Alves (2014) Here, the authors describe the concept of distributed long baseline as an algorithm, as opposed to hardware, solution for relative navigation of AUVs. Their approach is closely related to the one presented in this paper. However, in their case, the acoustic network was almost exclusively devoted to support the localization, with no constraints on the amount of data that could be transferred for localization purposes. Distances in Furfaro and Alves (2014) are limited to tens of meters as the objective is supporting multirobot tight formations. Experimental results are shown for a bottom-mounted four-modem acoustic testbed, the Littoral Ocean Observatory Network (LOON) (Alves, Potter, Guerrini, Zappa, & Lepage, 2014), with no mobile nodes, and hence no actual navigation. A cooperative localization algorithm that exploits the presence of an underwater acoustic network was proposed in Caiti, Calabro, Fabbri, Fenucci, and Munafò (2013a) and Allotta et al. (2015). In this case, the presence of mobile nodes was explicitly accounted for. However, the network was modified and adapted to fit the requirements of the localization algorithm since the system relied on dedicated solutions provided by the acoustic modems and by the USBL devices.

This work aims at exploiting the presence of networked communication to include services devoted to localization purposes, within an already existing and fully operational acoustic network. The addition of information must not interfere with the normal network operation and must make minimal use of acoustic communication for the purpose of navigation. In our mobile sensor network, localization data should be transmitted only when possible and when it does not affect higher priority messages. The approach proposed in this work does not limit the usability of more traditional acoustic positioning schemes. When they are present, the information provided can be seamlessly fused within the node's localization systems. Rather, the aim is that of showing how the inclusion of some dedicated information in a subset of the exchanged messages can greatly enhance the localization, without the need of dedicated instruments.

3. ADDING LOCALIZATION SERVICES TO ACOUSTIC COMMUNICATION

This section describes the integration of localization services to normal network traffic. The resulting architecture is similar to a long-baseline interrogation scheme, where the network itself is able to support AUV localization without requiring additional or dedicated instrumentation. This is similar to what has been discussed in Munafò et al. (2014), where the authors showed in postanalysis how to run a network-enabled localization algorithm.

Most acoustic navigation systems are based on measuring, at the level of the acoustic modem, the two-way time-of-flight (TOF) between transponders, so to convert this time into distances using measured or estimated sound speed values. For this to work, an acknowledgment is required to be sent from all the receivers to the transmitter. While no absolute precision clock is required for TOF measurements, the disadvantage is that the overall update rate for each vehicle decreases as $1/N$ in an N vehicle environment: Each node must interrogate the network to obtain a two-way TOF measurement between it and all replying nodes. Furthermore, when a Time Division Multiple Access (TDMA) Medium Access Control (MAC) scheme is used in the network, this method becomes extremely inefficient as it becomes necessary to allocate additional guard times for the transmission of the reply (or of an acknowledgment) from the interrogated node to the interrogator. Note that this approach worsens with the distance between the nodes since it takes more time for the acknowledgment to get back to the interrogator. This limits the types of localization devices that can fit within such a communication network, for example, USBL devices, which rely on acknowledgments to calculate their distance from a remote transponder, cannot be used. The usage of synchronized clocks scales to a multinode environment (all listeners can calculate the TOF with the interrogator at once). The price to pay in this case lies in the need for dedicated and high-precision clocks able to support the synchronization needs.

The approach proposed in this work uses a third alternative, based on asynchronous exchange of messages. According to this scheme, each node does not need to have a synchronized clock, as long as the acoustic modem is able to provide the time of transmissions and receptions, and information on its local clock is included in some of the packets. Figure 1 shows a two-way message exchange (message round trip) between two nodes, `A` and `B`. At time t_0^A, node `A` transmits its message to node `B`, which receives the message and saves the time of reception according to its local clock t_1^B. Node `B` cannot transmit its reply at once (e.g., the network uses a TDMA MAC protocol) and has to wait until time t_2^B to send a new message. When this message is sent, it includes in the payload the time of the message reception t_1^B and the current time of message transmission t_2^B. Finally, at time t_3^A, node `A` is notified about the time of reception t_3^A

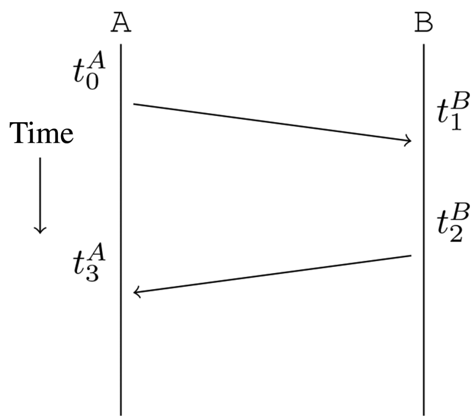

Figure 1. Network-based two-way message exchange or message round trip between two nodes. At time t_0^A, node A transmits its message to node B, which receives the message at t_1^B according to its own local clock. Node B replies at time t_2^B sending the time of the message reception t_1^B and the current time of message transmission t_2^B. When node A, at time t_3^A, receives this message, is able to calculate the round trip time of the message exchange.

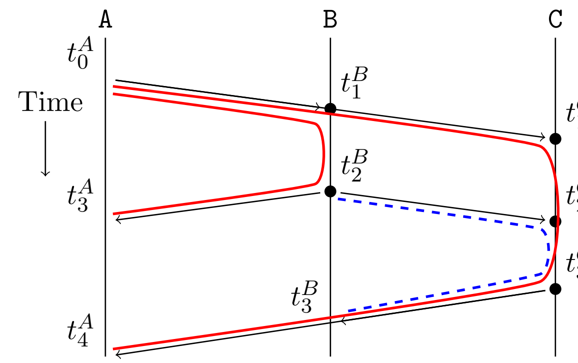

Figure 2. Message round trips in a three-node network. The two-way message exchanges have been indicated with connecting lines (solid, red line when node A is the initial interrogator; dashed, blue line when node B is the initial one). The data to be transmitted to the other nodes to complete the cycle are marked with filled black circles. These data scale linearly with the number of nodes. Node C, which, in this example, is the last node to respond, has to transmit three time stamps: two reception times and one transmission time stamp. The two-node example of Figure 1 corresponds to the top-left initial message round trip between A and B.

and reads from the message payload the two time stamps t_1^B and t_2^B. At this point, node A can calculate the message round-trip-time:

$$rtt_{AB} = t_3^A - t_0^A - \left(t_2^B - t_1^B\right). \tag{1}$$

Combining this information together with a measurement or an estimation of the sound velocity profile of the local water column makes it possible to calculate the range. When more nodes are present, this scheme can be scaled appropriately as shown in Figure 2 for a three-node network. No assumption is made on specific hardware requirements since no stable-precision clock is necessary. Moreover, the approach is independent of the specifics of the implemented acoustic network, and it is able to readily scale with the number of nodes. The price to pay is that local clock data must be added to each (localization) packet, slightly increasing the communication overhead. The amount of data that must be included scales linearly with the number of nodes. As shown in Figure 2, two nodes require two time stamps to be transmitted, that is the time of reception t_1^B and the time of transmission t_2^B (2×32 bits without data compression), three nodes require three time stamps (two reception times t_1^C, t_2^C from the two other nodes, and one time of transmission t_3^C), and so on and so forth. Note nonetheless, that it is easy to optimize the amount of data to be transmitted. One possible option is to only send one absolute time stamp of 32 bits and then to encode relative time from the first one, and/or to use data compression as shown in Schneider and Schmidt (2010). No matter the efficiency of the encoding though, for some scenarios, this communication overhead might impact too much on the capacity of the network, and not be tolerable for acoustic networks whose main objective is communicating application data rather than being a mere support for navigation. In this case, the proposed approach can still fit inside the network structure. In fact, it represents an additional network layer, that can be optimized to add the required data only when needed, as, for example, when the localization accuracy is lower than a prespecified threshold. The localization service could therefore be activated on-demand by optimizing the bandwidth used for localization with respect to the specific mission objectives.

3.1. Remarks

- When the transmission of the reply (see Figure 1) at time t_2^B can be done right after the reception of the request ($t_2^B - t_1^B \simeq TAT$, turn-around time of the instrument) the method reduces to something very similar to a traditional LBL implementation.
- The resolution of the range measurements is limited by the relative clock drift within a network-based two-way message exchange and depends on the available hardware. When no high precision clocks are used (i.e., those available in standard embedded computers), this drift could be as high as 60 ms h^{-1} (Vermeij & Munafò, 2015). In the case of a TDMA-based network with a 60-s frame, this limits the resolution to 1.5 m.
- The relative motion of the nodes during a message round trip might introduce a ranging error due to the possibly long time between the interrogation and its reply (see Figure 2). In this case, each node might include a

dynamic estimate of the motion of its remote counterpart or additional information may be available from the acoustic hardware (e.g., Doppler velocity made available from the acoustic modem when a message is received) to reduce the error.

- The way and frequency at which the nodes are able to respond to an interrogation ultimately depends on the MAC protocol of the network. In this respect, the number of network nodes may affect the performance of the MAC and in turn influence the overall range estimation error. For instance, in a TDMA-based access control scenario, the delay required for a node to respond to an interrogation depends on the node position in the TDMA transmission schedule. However, if a different MAC is used (e.g., ALOHA; Petroccia, Petrioli, & Sotjanovi, 2008), the nodes might not need to wait for a long time before replying, or multiple replies can be appropriately scheduled not to have collisions at the receiver (Anjangi & Chitre, 2016), reducing the message TAT and limiting the impact on the range estimation.
- The range measurement calculated with the proposed interrogation scheme can be associated with different positions of the interrogated node, and different choices might lead to different time association errors. With reference to Figure 1, one valid option is that of using the average position of the replying node `B` between the reception of the interrogation t_1^B and its associated transmission t_2^B. One alternative option is that of using the position of `B` at time t_2^B, as available when the node transmits its reply. This work uses this latter option as it has the advantage of requiring the shortest queue of historic states for the EKF, hence reducing the memory footprint of the filter.

4. EXTENDED KALMAN FILTER FOR NAVIGATION

An EKF is used to fuse the network-produced range measurements with the local navigation data from the vehicle: surge speed and heading. These are odometry data that are likely to be available also on vehicles with low-cost inertial systems. The surge speed can be measured using flow sensors or can be estimated based on dynamic models (Ferri, Manzi, Fornai, Ciuchi, & Laschi, 2015). The heading is easily available using compasses or Attitude and Heading Reference Systems. Despite its limitations (e.g., Gaussian unimodal estimation, sensor noise represented as zero mean, white noise), the EKF was chosen, in this work, as navigation filter due to its widespread usage in commercial AUVs as well as in most of the cooperative navigation methods (Bahr, Walter, & Leonard, 2009b), and because of its limited computational burden, and ease of implementation on most CPUs. Alternative approaches that overcome these limitations have been proposed, and the reader is referred, for instance to, Bahr, Leonard, and Fallon (2009a); Allotta et al. (2016); Paull, Seto, and Leonard (2014b); Walls, Cunningham, and Eustice (2015) and references therein.

In what follows, the position estimation problem is reduced to that of X–Y horizontal plane dynamics only: it is assumed that each vehicle is equipped with a pressure depth sensor of sufficient accuracy such that, at each time stamp k, slant-range pseudoranges can be projected onto the horizontal plane (Fallon et al., 2010):

$$z_k = \sqrt{z_{3D,k}^2 - (depth_{i,k} - depth_{j,k})^2}, \tag{2}$$

where $z_{3D,k}^2$ is the three-dimensional (3D) range between two nodes, and $depth_{i,k}$, and $depth_{j,k}$ is the depth of node i and j, respectively. Furthermore, each vehicle shares its depth with the other nodes including this information into the payload of an acoustic message.

In our typical mission environment, where the horizontal distances between the nodes are of several kilometers, and the depths are of the order of 100 m, the horizontal plane simplification is a safe assumption. The sound speed profile is assumed to be locally homogeneous within the prescribed bounding box of vehicle operations. This implies that TOF measurements can be converted to pseudoranges via a constant scaling by sound velocity. Each vehicle runs its own local navigation filter to predict its position (based on dead reckoning) and corrects this prediction using the ranges produced by the network. Range measurements are considered as made at the end of the corresponding message round trip t_3^A (Figure 1).

Finally, no assumption is made on the length of the underwater missions since the described method does not rely on synchronous clocks or periodic resurfacing to obtain GPS fixes.

4.1. Vehicle Process Model

Denoting the position and heading of the ith vehicle at time k as $X_{i,k} = [x_{i,k}, y_{i,k}, \theta_{i,k}]^\intercal$, where $(x_{i,k}, y_{i,k}, \theta_{i,k})$ represents the transducer position and heading in a locally defined Cartesian coordinate frame (e.g., Universal Transverse Mercator (UTM) System coordinates), the resulting kinematic model used in the prediction steps of the filter is:

$$X_{i,k+1} = \begin{bmatrix} x_{i,k+1} \\ y_{i,k+1} \\ \theta_{i,k+1} \end{bmatrix} = \begin{bmatrix} x_{i,k} + \Delta_k \cos(\theta_{i,k}) u_{i,k} \\ y_{i,k} + \Delta_k \sin(\theta_{i,k}) u_{i,k} \\ \theta_{i,k} + \Delta_k w_{i,k} \end{bmatrix}, \tag{3}$$

where u is the surge speed of the vehicle and w its angular velocity (calculated, for example, from consecutive readings of the vehicle's heading), and Δ_k is the sampling step. It is assumed that every node i maintains a vector $X_{i,k}$ that contains an estimate of its position, and the associated covariance matrix $P_{i,k}$ that describes the uncertainty of that estimate. Whenever the vehicle receives a new measurement (u, w) from its dead-reckoning system, it propagates forward its current estimate using the model (3) and updates the uncertainty using the Kalman filter equation:

$$P_{i,k+1} = A_{i,k} P_{i,k} A_{i,k}^{\mathsf{T}} + Q_{i,k}, \tag{4}$$

where $A_{i,k}$ is the Jacobian matrix of partial derivatives of the state (3), and $Q_{i,k}$ is the process noise matrix. This dead-reckoning estimate is combined with the network-produced range measurements, node positions, and covariances to produce a corrected position estimate and to bound the uncertainty.

4.2. Update Step

When, at time k, node i completes with node j one message round trip, it obtains the range measurement z_k, and receives from j its estimated position $X_{j,k}$ and uncertainty $P_{j,k}$ (see Section 5.2 for specific implementation details). For range-only measurements, the nonlinear measurement function between node i and node j is given by

$$h = \sqrt{(x_i - x_j)^2 + (y_i - y_j)^2}. \tag{5}$$

The correction step is then obtained by linearizing the previous model as well as the range measurements made from the network-based interrogation scheme, producing the following measurement residual equation:

$$y_k = z_k - \mathbf{H_k} \left\| X_{i,k} - X_{j,k} \right\|, \tag{6}$$

where z_k is the range measurement and $\mathbf{H_k}$ is the Jacobian measurement matrix:

$$\mathbf{H_k} = \left[-(x_{j,k} - x_{i,k})/\hat{z}_k, -(y_{j,k} - y_{i,k})/\hat{z}_k, 0 \right], \tag{7}$$

with $\hat{z}_k$ being the range between the nodes, that is, $\hat{z}_k = \sqrt{(x_{i,k} - x_{j,k})^2 + (y_{i,k} - y_{j,k})^2}$. The complete update phase of the filter is then

$$X_{i,k}^{+} = X_{i,k} + \mathbf{K_k} y_k, \tag{8}$$

where $\mathbf{K_k} = P_{i,k} \mathbf{H_k}^{\mathsf{T}} S_k^{-1}$ is the Kalman gain, with $S_k^{-1} = \mathbf{H_k} P_{i,k} \mathbf{H_k}^{\mathsf{T}} + \Sigma$. Σ is the range measurement noise matrix, which is defined as

$$\Sigma = \sigma_r^2 + \mathrm{tr}(P_{j,k}), \tag{9}$$

where σ_r^2 is a statically defined measurement variance as obtained for instance from historical data, and $\mathrm{tr}(P_{j,k})$ is the trace of the uncertainty matrix as received from node j. The second part of Σ makes it possible for the filter not only to include the uncertainty of the range measurement but also the uncertainty of the position of the remote node from which the measurement was received. In this way, the filter is able to reduce its confidence when integrating measurements coming from nodes that do not have access to GPS. This becomes especially important when a network is composed of multiple nodes that do not have access to absolute position information, and particular care must be taken to maintain the filter consistent. More specifically, when one robot `A` uses the position estimate of another robot `B` to update its own position, their estimates become correlated possibly leading to an overconfidence in the resulting estimation if this cross-correlation is not accounted for. Various methods have been devised to formally address the problem. In Arambel, Rago, and Mehra (2001), the authors propose a Covariance Intersection algorithm to distributively compute an upper bound on the filter covariance matrix. An algorithm, specifically designed for the underwater scenario, has been presented in Bahr et al. (2009b) where a bank of filters is maintained on each vehicle to track the origins of the measurements and not to use information more than once. More recent methods, such as Paull et al. (2014b) and Walls et al. (2015), are based on graph-based SLAM frameworks to implicitly handle the correlation when relative localization data are shared in a robotic network. These works aim at tailoring their approach to the limitations of the acoustic communication medium (i.e., low bandwidth and unreliability). The approach proposed herein realizes a trade-off between the amount of information that must be transmitted (only the trace of the covariance matrix is communicated together with the node position), the computation load (no additional filters or dedicated algorithms are needed), and the ability of the filter to output a consistent estimate. Moreover, as it will be described in the following sections (Section 5), the measurement variance (9) can be seamlessly fused within commercially available navigation filters that are usually developed to have LBL-like inputs (i.e., beacon position, range, and associated uncertainty). The implicit assumption that we are making is that there will be enough anchor points with GPS access with which the AUVs can bound their position uncertainty. In our specific scenario, where the AUVs are deployed within a multinode network where most of the assets have a surface expression (i.e., GPS) this assumption is not too restrictive. When this is not the case, different approaches should be considered.

The EKF described in (3)–(8) is augmented to have a fixed-length queue of historic states for the most recent n sampling steps: $\mathbf{X_{i,k}} = [X_{i,k}^{\mathsf{T}}, X_{i,k-1}^{\mathsf{T}}, ..., X_{i,k-n}^{\mathsf{T}}]^{\mathsf{T}}$. This allows to account for the delays between the range measurements and the reception of the remote beacon position. Note that when only the flow velocity is available, the model (3) can be further augmented to estimate the water current (Fossen, 2011). A simpler alternative is to directly increase the uncertainty of the model tuning the process noise (e.g., from historical data). This last approach is the one that it has been used in this work.

5. FIELD TRIALS

The proposed navigation system was tested during the activities of the COLLAB–NGAS14 experimental campaign. The sea trial was held from October 19, 2014 to October 31, 2014, off the west coast of Italy. The goals of the trial

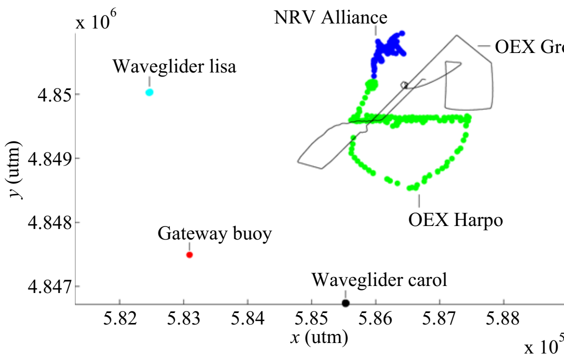

Figure 3. Platforms deployed during the COLLAB–NGAS14 campaign. Two OEX AUVs (OEX Groucho and OEX Harpo) were used as mobile assets; four fixed nodes equipped with acoustic modems where also deployed: two wave gliders, one gateway buoy and one additional node was setup on board the NRV *Alliance*.

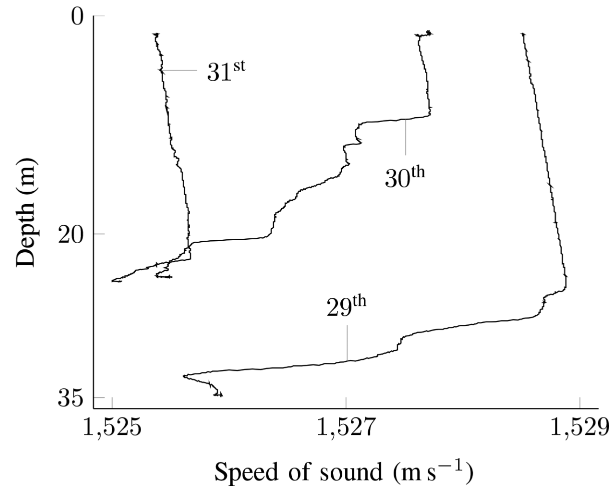

Figure 4. Sound velocity profiles measured on October 29–31, 2014 (Vermeij & Munafò, 2015). Note the general low variability in the profiles. On October 31, 2014, when the activity described in this work took place, the sound speed was nearly constant throughout the water column.

ranged from testing new AUV autonomy, to sonar signal processing, and to AUV navigation and localization. For the purpose of this work, we focus on the activities that took place on October 31, 2014.

5.1. Site Description

The site of the AUV navigation and localization testing, shown in Figure 3, is located near 43.7754 N, 10.03333 E, off the coast of Tuscany, Italy. The entire area of operation is a 7.5 km × 7.5 km square. Water depth in the area goes gradually from around 25 m (northeast part of the area) to around 60 m (southwest region). This water depth is convenient as it allows the AUVs to have DVL bottom lock throughout the mission. This provides an accurate navigation solution that can be used as ground truth for performance comparisons. The area was characterized by the presence of a fair water current of around 0.5 ms^{-1} moving from north to south.

The sound velocity profile, as measured at a location close to the northeast corner of the area from October 29 to October 31, 2014, is shown in Figure 4. Note that on October 31, the sound speed is nearly constant throughout the water column.

5.2. Experimental Setup

The deployed network was composed of one moored gateway buoy, two wave gliders (Carol and Lisa) (Liquid Robotics, 2015), two CMRE OEX AUVs and one additional node which was deployed off the NRV *Alliance* (see Figure 3).

The two AUVs, OEX Groucho and OEX Harpo, are vehicles of 4.5 m length and a diameter of 0.53 m, which can operate at the maximum depth of 300 m. Their maximum speed is 3 kn, and their battery endurance is about 16 h. OEX

Figure 5. OEX Groucho deployed from the NRV *Alliance*. The acoustic modem with the down pointing transducer is visible in the front.

Groucho, during its deployment from the NRV *Alliance*, is shown in Figure 5.

Each OEX is equipped with a main computer and with a configurable payload section. The main computer directly commands the vehicle and maintains navigation. The payload section is used for MOOS-IvP autonomous decision making (Ferri et al., 2014), on-board signal processing (Canepa, Munafò, Murphy, Micheli, & Morlando, 2015), and to run all the necessary network components. The two computers are integrated together using a “front-seat driver/back-seat driver” paradigm, as shown in Figure 6. According to this paradigm, there is a clear separation of the vehicle control (front seat) from the vehicle autonomy

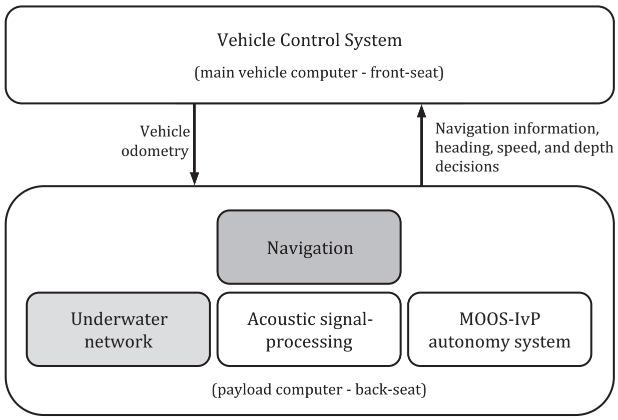

Figure 6. The back-seat driver paradigm as implemented onboard the OEX. The key idea is the separation of vehicle autonomy from vehicle control. The payload computer (back-seat) includes the autonomy system and the network-based navigation, providing heading, speed, and depth commands to the vehicle control system (front-seat), together with navigation information. The vehicle control system executes the control, for example, position, heading, and speed, and passes back odometry readings to the autonomy system.

(back seat) (see, for instance, Benjamin, Schmidt, Newman, & Leonard, 2010). The autonomy system provides heading, speed and depth commands to the vehicle control system. The vehicle control system executes the control and passes navigation information, for example, position, heading, and speed, back to the autonomy system.

The accuracy of these data depends on the specific scenario, and on the navigation and control devices with which the vehicles are equipped. For the purpose of this experiment, the vehicles were instrumented with a typical suite of navigation sensors including pressure sensor, DVL, and a gyro for attitude. The DVL, which, in the area of operations, had continuous bottom lock, was set up to measure the speed over ground and the water velocity at a depth of 5 m below the vehicle, and to provide them to the AUVs as two separate data streams, that could be accessed independently. Both vehicles were equipped with commercial INS, able to fuse together the desired set of navigation inputs, and to produce a navigation solution for the front-seat computer (i.e., front-seat navigation filter). The INS was used in a different way, in each AUV. OEX Groucho's INS was set up to read the pressure sensor, the on-board gyro, and the DVL-produced speed-over-ground. The position drift of OEX Groucho was, with this configuration, $\sim 0.05\%$ of the distance traveled, that is, 0.5 m every 1 km. This accuracy was cross-validated using GPS measurements and the HiPAP acoustic positioning system (Kongsberg Maritime, 2015), available on the NRV *Alliance*, and able to localize the vehicles up to a range of $\sim$1 km. This setup allowed the vehicle to reliably navigate without using the network-produced range measurements. For this experiment, this front-seat navigational estimate was periodically transmitted acoustically from OEX Groucho to the rest of the network. This was done to use OEX Groucho as an additional anchor point (its navigation ability was comparable to having access to GPS), and it made it possible to reduce the operational risk for the other vehicle OEX Harpo, which, as will be explained in the next paragraph, was navigating without bottom-lock while relying only on network-generated measurements. At the same time, a separate Kalman filter was run on OEX Groucho's back-seat computer as described in Section 4. This filter used the vehicle's velocity as measured with respect to the water and the vehicle's heading as odometric input for the prediction phase, and the network range measurements as correction data.

A different setup was used for OEX Harpo. In this case, the front-seat computer ran the navigation filter reading INS data, water velocity instead of ground velocity from the DVL (hence it is subject to water current errors) and the network range measurements. This is equivalent to a deep water navigation scenario where the DVL cannot get bottom lock, and the network-based navigation aid has the greater benefits. Since, in this case, there is no high-precision navigation available, HiPAP measurements were used as position ground truth. The usage of OEX Groucho as an additional anchor point for this vehicle was useful to increase the number of range measurements available with an absolute positioning and minimum uncertainty, reducing the risk for this vehicle to move out of the acoustic communication coverage which would mean to navigate underwater with no communication and poor navigation.

Having different setups for the vehicles made it possible to test different filters and configurations in the limited experimental time available. A summary of the front-seat/back-seat configurations for the AUVs is reported in Table I; a schematic is shown in Figure 7. Note also that, this specific experimental configuration allowed the vehicle filters not to use the same information more than once.

During the experiment, OEX Groucho was commanded to navigate at 25 m depth; OEX Harpo was kept at 15 m depth. The wave gliders were station keeping throughout the trial. The modems of the Gateway and of the NRV *Alliance* were deployed at a fixed depth of 25 m; wave glider modems at 6 m depth. All surface assets were equipped with a GPS receiver used for measuring transducer position. All nodes were equipped with the EvoLogics 7–17 kHz acoustic modem (Evologics GmbH, 2015). The specific structure of the acoustic network is described in the next section.

5.3. The Acoustic Network

5.3.1. Physical Layer: The Acoustic Modems

The physical layer of the underwater communication network was supported on EvoLogics GmbH 7/17

Table I. Summary of the front-seat/back-seat set-ups on both vehicles.

	Front-seat Navigation	Back-seat Navigation
OEX Groucho	Commercial navigation filter fusing INS data and DVL speed-over-ground	EKF reading vehicle heading and DVL speed-over-water for the prediction phase, network-produced range measurements as correction data
OEX Harpo	Commercial navigation filter fusing INS data, DVL speed-over-water, and network range measurements	No navigation filter. The back-seat computer run the acoustic network stack to produce range measurements.

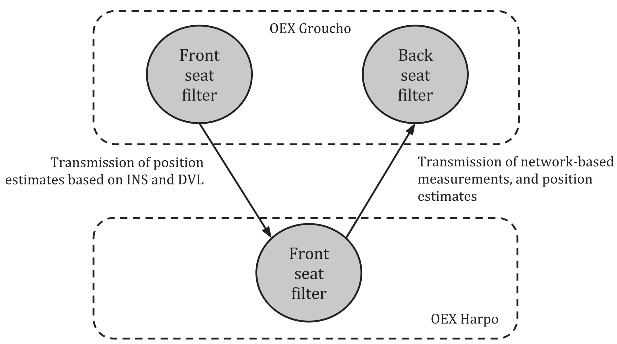

Figure 7. Schematic of the navigation filters running on the AUVs, together with the main information exchanged between OEX Groucho and OEX Harpo. OEX Groucho transmitted acoustically the position estimated by the front-seat navigation filter, while fusing the network-produced measurements and node's positions in its back-seat filter. OEX Harpo was run with the front-seat filter with no bottom-lock and receiving network calculated range measurements.

low-frequency acoustic modems (Evologics GmbH, 2015). These modems are characterized by a hemispherical transducer beam pattern and work in a frequency band between 7 and 17 kHz. The modem transmission power is settable up to a level of 186 dB re 1 $\mu Pa@1m$, which allows, in nonrefractive environments, a working range of around 8 km. The modems were set up to use the so called "instant message" communication. This communication method allows the modem driver to have maximum control over the modem behavior and transmission scheduling. No connection establishment procedures are required, and unicast message exchange as well as broadcast messaging to all devices at once are permitted. The maximum achievable bit rate is 976 bps, including packet headers and error correction. The maximum permitted message size is 64 bytes, and this is transmitted acoustically in 1 s. The acoustic modems are able to provide to the upper layers of the network the time of acoustic transmissions and receptions (Kebkal, Kebkal, & Bannasch, 2011). Using this information, it becomes possible to associate transmission and reception time stamps and hence to calculate message round trip times.

5.3.2. MAC Layer: A TDMA Protocol

The network is based on a TDMA scheme to handle the shared communication medium, that is the acoustic channel. According to this scheme, different communication nodes share the same bandwidth but they avoid conflicts by transmitting at different times. Time is divided into slots, and each node is assigned a slot where it has to concentrate all its communication burden. The set of slots that include all the vehicles is usually called a frame, and it repeats when it reaches its end. TDMA provides collision-free communications with acceptable utilization of the available bandwidth and permits, in the case of networks composed of a limited number of nodes, to have a better network throughput in terms of average transmission delays and energy requirements with respect to more complicated networking mechanisms (Caiti, Calabrò, & Munafò, 2012b). A typical TDMA scenario for the CASW network is composed of six slots, one per node, with the AUVs' slots of length 12 s to permit the transmission of five messages of 64 bytes up to a distance of 8 km, and shorter slots of 6 s allocated to the Command and Control (C2) to send mission commands to the vehicles and to gateways and wave gliders, which mainly need to send their position to the vehicles. The overall TDMA frame is 66 s, including gap periods to allow for the acoustic signal to travel to all destinations. The length of the TDMA frame is statically defined based on the maximum number of nodes, as known a priori, before deployment.

A flooding routing layer may be used for multihop transmissions (Caiti et al., 2012a, 2013b). According to this scheme, the nodes need not to be within broadcast range of one another. However, routing requires a great deal of communication overhead. For this reason, in our scenario, where the application layer is eager for bandwidth, this layer is not utilized if not absolutely necessary.

5.3.3. The Queuing System

In acoustic-based networks, the desired throughput is almost always above the available capability. To optimize the channel usage, the CMRE acoustic network uses a priority-based queuing system (Schneider, 2013). The message priority is a combination of two parameters: the importance of the message and its time to live. The queuing system plays an important role for the network interrogation cycle since it is responsible for scheduling message transmissions.

5.3.4. Network Upper Layers: The Mission-Oriented Operating Suite Middleware

The network upper layer is based on the Mission Oriented Operating Suite (MOOS) architecture (Benjamin, Newman, Leonard, Newman, & Schmidt, 2009), (Benjamin et al., 2010). MOOS is a publish/subscribe framework that is used for interprocess communication. The core component of the MOOS is the so-called MOOSDB, a central server that acts as a bulletin board that holds the current state of the variables of the running processes, that is, on-board signal processing, communication, navigation, and autonomy processes. Processes can subscribe to and/or publish variables to the MOOSDB to exchange information. When an application needs to send an acoustic message, it publishes its data into a MOOS variable. From the MOOS variable, the data are passed on to the lower levels of the network to be acoustically transmitted. On the other side of the link, the received data are published in the receiver's MOOSDB. From the MOOSDB it is accessed by the receiver's applications. MOOS applications might trigger asynchronous transmission of acoustic messages, such as when active sonar measurements are present (Canepa et al., 2015; Ferri et al., 2014), or they might schedule periodic messages as, for instance, when a node needs to transmit its periodic status report. This latter message is used to monitor the vehicle operation and includes its position, velocity, and associated uncertainties.

The MOOS system, extended with the Interval Programming (IvP) module, is also used to enable behavior-based autonomy on the AUVs. IvP is a mathematical interval programming technique, which permits the combination of several objective functions produced by different and often competing behaviors to swiftly determine a combined solution (Benjamin, 2002).

5.4. Network Interrogation Cycle

Although the proposed network interrogation cycle is independent from the network structure, for the purpose of this work, some implementation details have been constrained based on the available network. The acoustic modems are considered to be set up for broadcast transmissions, so that each node can transmit to everyone else that is within its maximum communication range. This is the typical operational setup for our network since it reduces the number of messages to be transmitted. One message round trip, which is conceptually composed of only two messages, has been divided into three sequential messages, plus one additional message required to share the most recent (estimated) position and uncertainty. By relying on specific modem hardware (e.g., automatic encapsulation of transmission times), it might be possible to reduce such a number of messages to two, but this would violate our software-defined architecture. Figure 8 shows the messages required to complete an interrogation cycle in a two-node case. Let us call t_0^A the time reported by the modem to the host computer A when an acoustic packet is sent. This packet is received at modem B at time t_1^B. Given the TDMA communication scheduling, modem B cannot reply at once to modem A and has to wait for its transmission slot. At time t_2^B modem B's slot starts, and it sends a first packet which includes the t_1^B time stamp as payload. This first transmission generates the time stamp t_2^B. To complete the interrogation cycle, node B encodes this transmission time stamp as a payload of a third message, which is sent at time t_4^B. Finally, node B shares its most recent (estimated) position and uncertainty, encoding another message, which, in general is sent at a different time t_6^B. The transmitted position relies on the status messages generated by the node's application layer (see Section 5.3.4). No new dedicated position messages are generated by the network localization system not to increase the bandwidth consumption.

In this implementation, time stamps t_1^B and t_2^B cannot be sent within the same acoustic packet since t_2^B is produced only once t_1^B is transmitted. Note, however, that this is only an implementation detail and that alternative solutions can

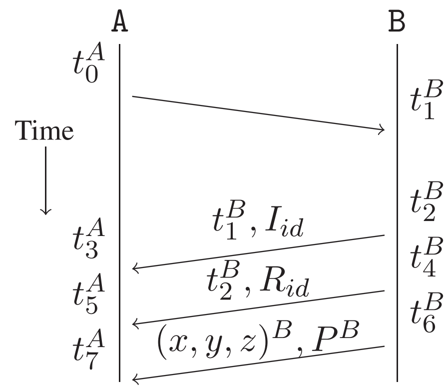

Figure 8. Implemented network interrogation cycle and sequence of messages exchanged. At t_0^A, node A transmits the interrogation request, which is received by node B at t_1^B. At t_2^B, node B send its first reply containing the reception time t_1^B. This packet is received at time t_3^A by node A. At t_4^B, node B transmits a second packet A containing the time t_2^B at which its previous packet was sent. The reception of this packet completes the network interrogation cycle. Finally, at time t_6^B, node B sends its position (x, y, z) and its uncertainty P^B to node A. I_{id} and R_{id} are the modem ids of the interrogator and the replier, respectively. While I_{id} must be explicitly included in one message to allow A to associate its request to the received reply, R_{id} is encoded automatically by the modem and does not require additional overhead.

be easily envisioned where one message could be used to include both time stamps (e.g., pre-scheduled transmissions where time stamps are known in advance). Time t_3^A is used as reception time to complete the message round trip. The node's location might fit either inside the packet containing t_1^B, inside the one containing t_2^B, or even in a third packet. The actual scheduling depends on the network queuing system, which also considers the availability and importance of other messages. To complete a network cycle, both t_1^B and t_2^B must be correctly received from node `A`. However, if the message with node's `B` position is lost, `B`'s last known position is used instead. While this has a minor impact for the fixed nodes, it might induce larger errors for the mobile ones.

When more than two nodes are present, a node might receive multiple interrogation requests and some more information must be transmitted to associate each transmission to each reception. Since the communications are broadcast, a node receiving an interrogation request (see Figure 8) must associate the reception time stamp t_1^B with the modem id, I_{id}, of the interrogator. The couple $\{t_1^B, I_{id}\}$ will be sent in the message containing the interrogation reply. When the interrogator receives a time stamp associated with its I_{id}, it can work out the association between its request and the response. Only if the source address of the message containing t_1^B corresponds to `A`'s node address, the received message can be associated with the transmission time t_0^A. Finally, each t_2^B must be associated with the address of the transmitting node, R_{id} (and the message $\{t_2^B, R_{id}\}$ is sent). This address R_{id}, in our implementation, is encoded automatically by the modem and does not require additional overhead. When all this information is correctly received, `A` can calculate the round trip time using Eq. (1).

5.5. EKF Initialization

The EKF linearizes the system state along the system trajectories. An initialization too far from the actual state might cause the algorithm to become unstable. For this reason, a careful initialization must be done. The front-seat computer, which is, in our vehicles, the only one that has access to GPS measurements (these are used for the initialization of the front-seat navigation filter), signals the back-seat computer when it is giving up the control of the vehicle. This corresponds, in our mission setup, to a moment in which the vehicle is still on surface, with the front-seat filter able to produce very precise navigation data using the GPS. This information is used to initialize the back-seat vehicle state and covariance. Once the vehicle starts its mission, the accuracy of the front-seat-produced navigation fixes depends on the availability of DVL measurements. For the purpose of this work, after the initialization phase, navigation fixes from the front-seat are not used by the back-seat filter, while they are logged for performance comparison.

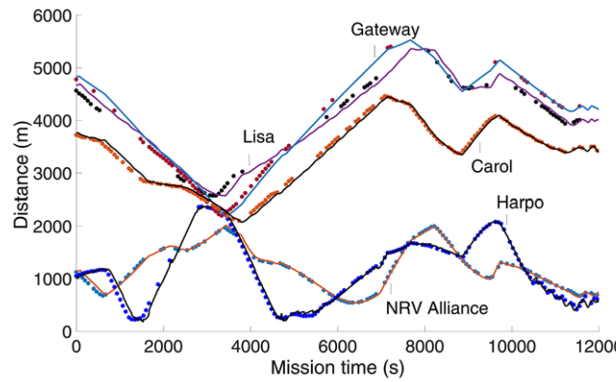

Figure 9. Distance between OEX Groucho and the other nodes. Colored filled circles represent the network calculated range. Lines report the range as obtained (depending on the node) from GPS and DVL-based IMUs. This is used as ground truth to evaluate the performance of the network-based navigation. Variation with time and with nodes is clearly visible, with periods of poor acoustic communication leading to poor ranging performance.

5.6. Experimental Results

This section describes navigation results obtained using data collected on October, 31, 2014.

OEX Groucho online navigation relied on the front-seat filter, which read INS data and DVL speed-over-ground. A separate EKF was running on the back-seat computer reading a subset of the navigation data (vehicle heading and speed-over-water to simulate deep water navigation), and using network-produced measurements as a means of limiting the navigation error. During the experiment, the value of the range measurement standard deviation σ_r was defined on the basis of past experimental data collected during the COLLAB13 sea trial (Munafò et al., 2014). More specifically, a value of $\sigma_r = 25$ m, considered representative for this setup, was used. The high precision front-seat navigation is used as ground truth for the back-seat one. The network-calculated distance between OEX Groucho and all the other five nodes of the network is shown in Figure 9. In the picture, continuous lines represent ground truth calculated using GPS for assets on surface and the front-seat inertial navigation for the AUVs. The network range measurements are shown as dots. Note the presence of long periods of time where no range measurements were available from some of the nodes. These were periods of poor acoustic communication, characterized by a high number of lost messages. Note how OEX Groucho had reliable communication with Wave Glider Carol (node 12), with the NRV *Alliance* (node 1) and with OEX Harpo, which allowed the network to produce range measurements throughout the mission. Worse communication was achieved with Wave Glider Lisa (node 11). Communication with the gateway was good for the first

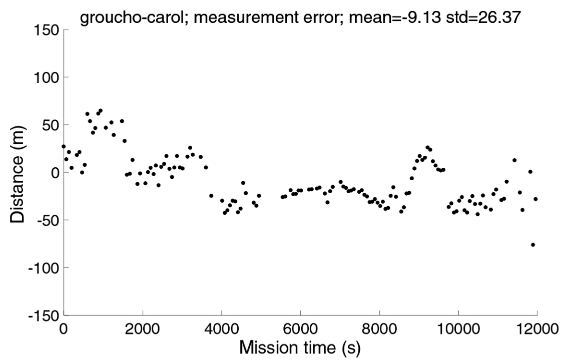

(a) OEX Groucho - Wave Glider Carol

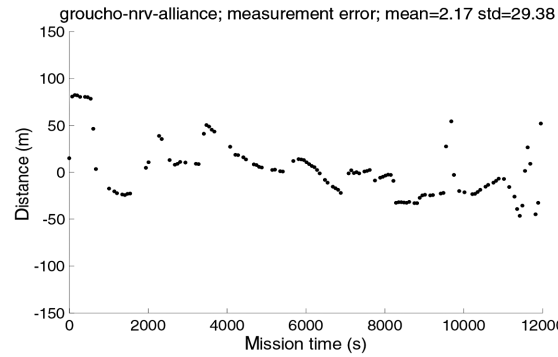

(b) OEX Groucho - NRV *Alliance*

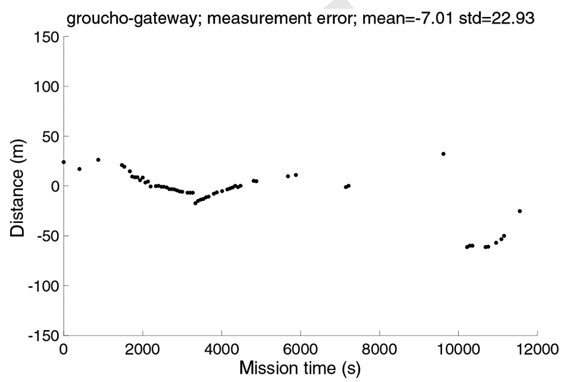

(c) OEX Groucho - Gateway

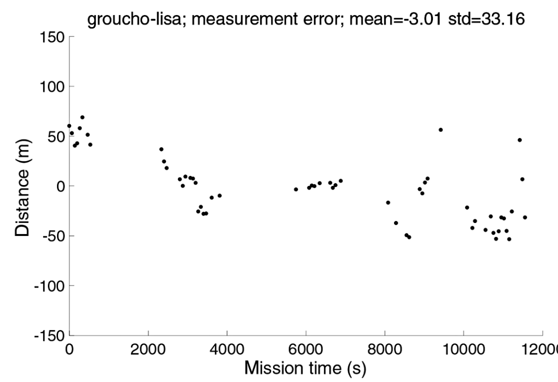

(d) OEX Groucho - Wave Glider Lisa

Figure 10. Network range measurement errors between OEX Groucho and the other nodes of the network. The average range error went from $\sim$ –9 to $\sim$ 3 m, and the standard deviation from $\sim$ 23 to $\sim$ 35 m. The maximum error was about 90 m, remaining below 50 m most of the time, regardless of the remote node. The mean and standard deviation for each node pair are given in the plot titles.

hour, and then dramatically poor. OEX Groucho's range measurement errors are reported in Figure 10. The average range error $\bar{\epsilon}$ went from $\sim$–9 to $\sim$3 m; the standard deviation from $\sim$23 to $\sim$35 m. The maximum error was about 90 m, remaining below 50 m most of the time, regardless of the remote node. Higher errors and a larger standard deviation was obtained for the NRV *Alliance*, which was located in shallower waters, and was subjected to more multipath. In this case, the more distorted signal affected the ability of the modem to correctly identify the start of the incoming signal. Furthermore, the modem on the NRV *Alliance* was lowered over the side with a floating cable and it was not rigidly attached to the ship. The motion of the ship and the resulting movement of the modem transducer may have influenced the accuracy of the range measurements. In general, however, the overall performance was quite stable regardless of the specific node pair.

The inputs, forward speed with respect to the water measured by the DVL sensor, and the vehicle heading, used by the back-seat EKF during the prediction phase, are reported in Figure 11. Note the noisy velocity measurements produced by the sensor. A hardware problem on the DVL affected the calculation of the water velocity and increased the noise level. The speed-over-ground, which was used by the front-seat filter but not by the EKF, was instead not affected.

Results of OEX Groucho's back-seat navigation are shown in Figure 12, where the front-seat DVL-based navigation (thin solid line in the figure) is compared with the back-seat one (bold dotted line). Note how the back-seat filter was able to correctly follow the actual vehicle navigation, correcting whenever new measurements were available. The corresponding navigation errors are reported in Figure 13(a) with a solid black line, together with the modem id of the node with which a network interrogation cycle was successfully completed [Figure 13(b)]. The vehicle was pinging all network nodes (node ids: 1, 3, 10, 11, 12) throughout the mission and was able to bound its navigation error to around 60 m. The resulting spatial uncertainty is shown in Figure 14 plotting the fourth root of the

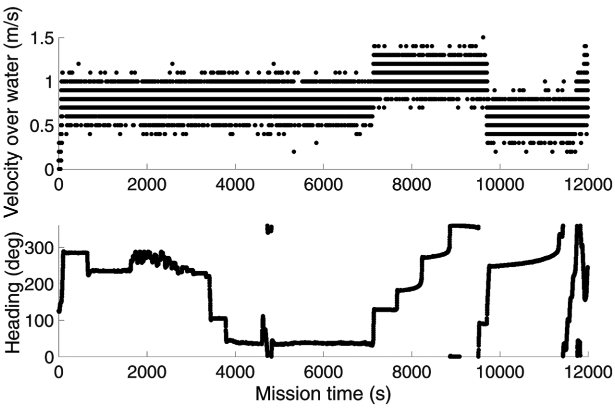

Figure 11. OEX Groucho's forward speed calculated with respect to the water, and heading during the mission. These values were used by the back-seat EKF during its prediction phase. Note the noisy velocity measurements coming from the DVL and caused by a hardware problem (diagnosed after the mission).

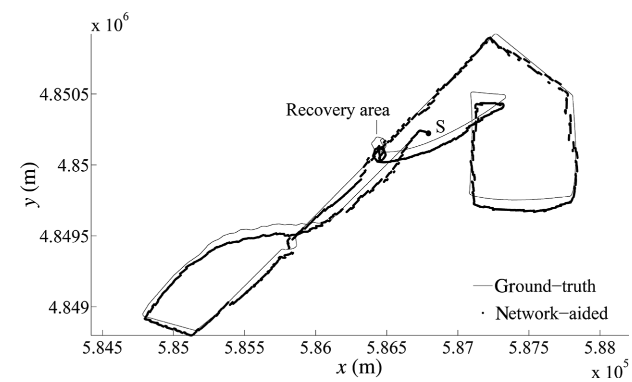

Figure 12. OEX Groucho navigation as produced by the back-seat filter using the acoustic network navigation system. Ground truth from the DVL-aided navigation is shown as a thin black line. Back-seat navigation is reported as bold black circles. The point where the mission started is indicated by the letter S. The recovery area is also indicated.

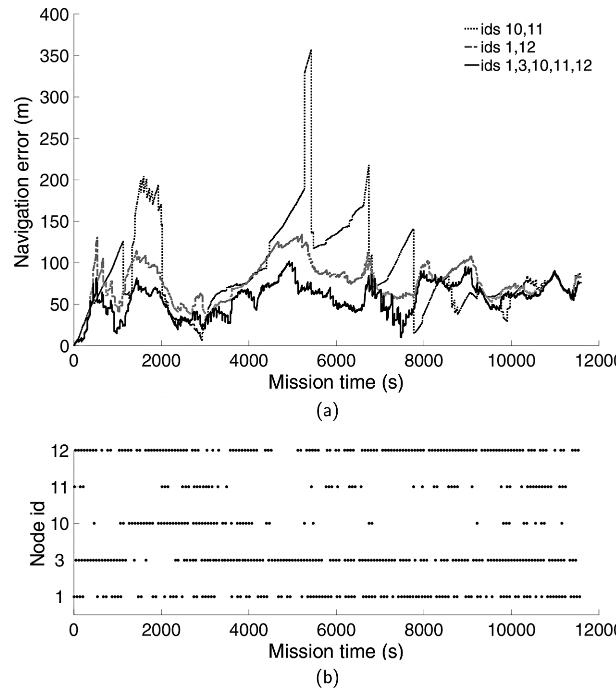

Figure 13. Top: OEX Groucho navigation error with varying number of network nodes. The ground truth to calculate this error is represented by the DVL-aided inertial navigation filter available in the front-seat computer of OEX Groucho. The picture shows the impact of the number of nodes used to increase the navigation accuracy. Toward the end of the mission, better communication performance was available and the error decreases regardless of the number of nodes used. Bottom: modem id with which OEX Groucho was able to complete a network interrogation cycle.

determinant of the x–y portion of the covariance matrix of the EKF filter (Webster et al., 2012). It is evident how the availability of network-generated range measurements reduces the uncertainty and keeps it bounded. If no range measurements are used, the spatial uncertainty grows without bound. This case is not shown in the picture, but the effect of a lack of measurements is clearly visible between mission time 6,800–7,750 s for the scenario in which OEX Groucho was only using nodes 10 and 11. During this period, the AUV was not able to complete network interrogation cycles and both the navigation error and the uncertainty quickly increased.

The same scenario was run in postprocessing, to quantify the vehicle navigation performance with a reduced number of network nodes and varying number of localization messages. Two cases have been analyzed, where the AUV could only ping two nodes out of five. A summary of these results is reported in Figure 13(a). The navigation performance depends on the number of nodes composing the network, and, even more importantly, on the number of successfully completed interrogation cycles. When good communication was available, the navigation accuracy obtained with only two beacons (nodes 1 and 12) is only marginally worse than the one obtained with five nodes. The main difference in this case is due to the fact that to complete an interrogation cycle with nodes 1 and 12, OEX Groucho has to wait for a longer time—nodes 1 and 12 are at the end of the TDMA cycle from OEX Groucho's perspective. When the communication becomes more sporadic (i.e., less interrogation cycles can be completed), the localization

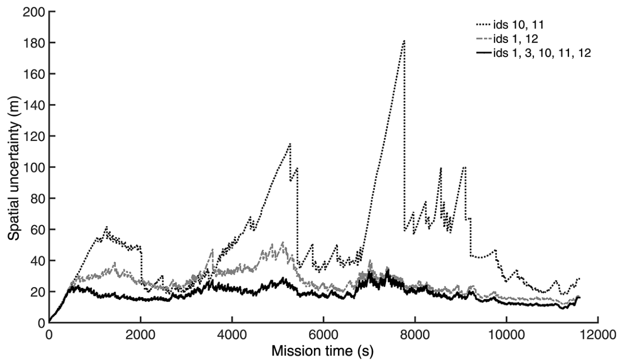

Figure 14. Spatial uncertainty of the back-seat navigation filter of OEX Groucho represented as the fourth root of the determinant of the x–y portion of the covariance matrix of the filter with varying number of nodes. The uncertainty is kept limited by the network-based range measurements. Note the rapid increase in uncertainty due to the lack of measurements between 4,500–5,300 and 6800–7750 s when OEX Groucho uses only two network nodes (ids 10 and 11). Note also that when the network is able to successfully complete the interrogation cycles, the filter is quickly able to reduce its uncertainty.

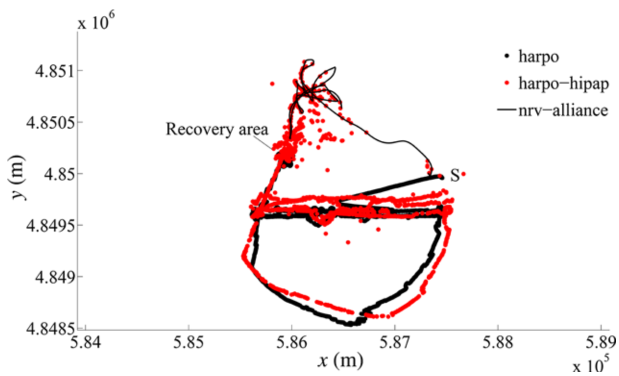

Figure 15. OEX Harpo navigation as done using the network range measurements directly in the front-seat filter. HiPAP position fixes are reported as red filled circles. OEX Harpo's front-seat solution is represented as black circles. The position of the NRV *Alliance* where the HiPAP was installed is shown as a thin black line.

performance decreases. This is the case of OEX Groucho using only nodes 10 and 11 as localization counterparts.

Note that, running the model (3), in the same conditions, but without network range measurements leads to an ever growing navigation error which is around 1.5 km at the end of the mission ($\sim$ 25% of the distance traveled).

A different kind of experiment was performed with OEX Harpo. In this case, the vehicle was set up to navigate while fusing, in real time, its odometric data (INS and DVL speed-over-water) with the network range measurements. Results of this trial are shown in Figure 15, compared to

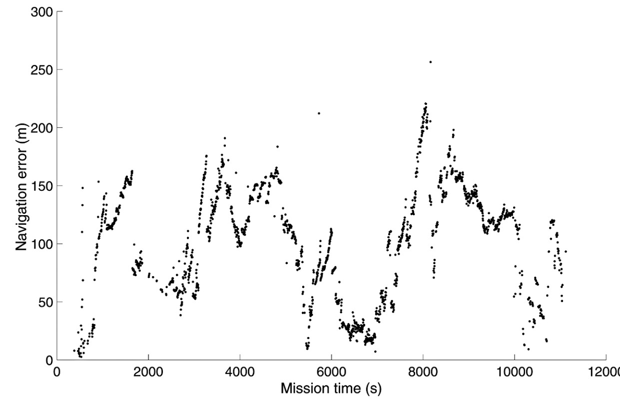

Figure 16. OEX Harpo navigation error between the vehicle front-seat filter output and the HiPAP acoustic positioning system. The HiPAP system was configured to have a maximum position update from the vehicle of 2 s. After 11,100 s from the mission start, the HiPAP system was not able to produce any more fixes on OEX Harpo.

position fixes obtained from the HiPAP acoustic positioning system mounted on the NRV *Alliance* and used here as ground truth. It is worth highlighting that several times the HiPAP system was not able to provide a correct navigation solution. This is visible in the picture as a cloud of points very close or even on top of the NRV *Alliance* position. During its mission, OEX Harpo was able to successfully use two nodes for the network interrogation cycle, OEX Groucho and Wave Glider Carol, whereas only few fixes were obtained from the other nodes. The navigation error obtained comparing the vehicle navigation to the one obtained from the HiPAP is reported in Figure 16. The associated spatial uncertainty, plotted as the fourth root of the determinant of the x–y portion of the covariance matrix is shown in Figure 17. The effect of the network aided navigation system in keeping the navigation error bounded is visible, with drops in the error when new range measurements were received.

5.7. Sources of Errors

In the Kalman filter, both the process noise and the measurement noise are assumed to be Gaussian with zero-mean. When this assumption is violated, it becomes a source of error for the filter. In this experiment, the only sensor that can be modeled as having Gaussian noise is the heading sensor of the vehicle. The water velocity measurements, coming from the DVL, had both a time varying bias and a noise that was not Gaussian. This was due to a sensor hardware problem diagnosed after the mission. Acoustic range measurements are not Gaussian distributed. This is due to a multiplicity of factors, including ray bending of the acoustic signal and erroneous range measurements due to multipath.

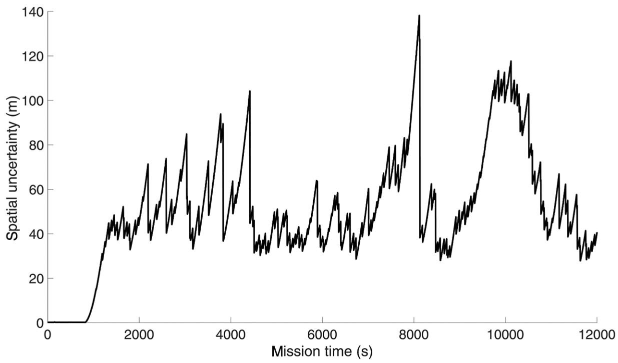

Figure 17. OEX Harpo spatial uncertainty calculated as the fourth root of the determinant of the covariance matrix of the front-seat navigation filter. The trajectory has bounded uncertainty as a result of the network produced range measurements. Without measurements the uncertainty raises quickly.

The sound speed, in this implementation, was considered as having a constant value of 1,525.3 ms^{-1}, everywhere in the area. This average value was obtained from a Conductivity Temperature Depth (CTD) profile done from the NRV *Alliance*, before starting the mission. When more variation is present, the usage of a time varying sound speed value, and of a range-dependent component for the range measurement model would help in reducing the errors (Casalino, Caiti, Simetti, & Turetta, 2011).

Another source of errors is represented by acoustic multipath. This can cause errors in the range measurements due to the fact that the acoustic signal bounces off the sea surface and/or the sea bottom possibly multiple times before reaching the receiver. In our case, the presence of multipath enhanced the multimodal distribution of the errors. Figure 18(a) shows the distribution of the innovations for the 142 range measurements between OEX Groucho and Wave Glider Carol made during the mission. Note the presence of multiple peaks in the distribution. Similar results are obtained for the other nodes as shown in Figure 18.

Moreover, the modem was mounted on the vehicle in the fore part of the hull, pointing downwards. This mounting influenced the overall performance, especially when the AUV moved away from its remote counterpart. In this case, the modem was shadowed by the vehicle hull and picked up the wrong multipath component.

Note also that the network interrogation cycle implemented for this trial was based on two simplifications. First, the remote nodes can send an updated position within the current transmission time slot, right after a message round trip is completed. This in practice might not always be the case. The network can in fact prioritize other messages for transmission within the current time slot transmitting the node position later or not transmitting it at all. When the position is postponed within the same time slot, this creates an error between the round trip time calculation and the associated position of the remote node. The magnitude of this error depends on the delay between the two messages and on the relative movement between the two nodes. If instead the message is not transmitted, a new range is produced and associated with the last known position of the remote node. Again, the induced error depends on the relative movement between the two nodes. Second, the propagation time used to calculate the distance between two nodes is considered to be half of the message round trip time. Although this can be a reasonable assumption for slow moving nodes or when the message round trip can be quickly finalized (e.g., short distances and reduced number of nodes in a TDMA scheme), in our case, this might not always be correct.

With reference to Figure 1, the round trip time between two nodes that are moving away from way from each other along a straight line, `A` and `B`, is

$$rtt_{\mathrm{AB}} = t_{\mathrm{AB}} + t_{\mathrm{BA}} \tag{10}$$

where

$$t_{\mathrm{AB}} = \frac{B_0 + v_{\mathrm{AB}}(t_1^{\mathrm{B}} - t_0^{\mathrm{A}})}{c} \tag{11}$$

and

$$t_{\mathrm{BA}} = \frac{B_2 + v_{\mathrm{AB}}(t_3^{\mathrm{A}} - t_2^{\mathrm{B}})}{c} \tag{12}$$

where B_0 is the initial position of node `B`, with respect to node `A`, which is considered the origin of the reference frame. B_2 is the position of `B` where it transmits the reply back to `A`. v_{AB} is the relative velocity between the two nodes, which is considered to be constant throughout the message round trip. c is the speed of sound in the water. Substituting, (12) and (11), into (10), we get the following expression for the round trip time:

$$rtt_{\mathrm{AB}} = 2\frac{B_0}{c} + \frac{1}{c}v_{\mathrm{AB}}(t_3 - t_0) \tag{13}$$

From (10), it is easy to see that, depending on the relative movement of the two nodes, one of the two components of the message round trip, t_{AB} or t_{BA}, can be a larger factor in the overall rtt. If the nodes are not moving with respect to one another, then of course, the rtt is simply the distance between the two nodes divided by the speed of sound c. When the nodes are moving, rtt_{AB} becomes a function of the relative velocities of the nodes and the period of time between the two way message exchange. In the implemented scheme, this has not been considered and the rtt is calculated as if the nodes have always a zero relative velocity.

Finally, in our application and experimental setup, the delays implied by the TDMA, while affecting the ranging performance, did not affect the navigation estimates significantly. As shown in Figure 13(a), in the worst scenario analyzed, when OEX Groucho was using only two beacons

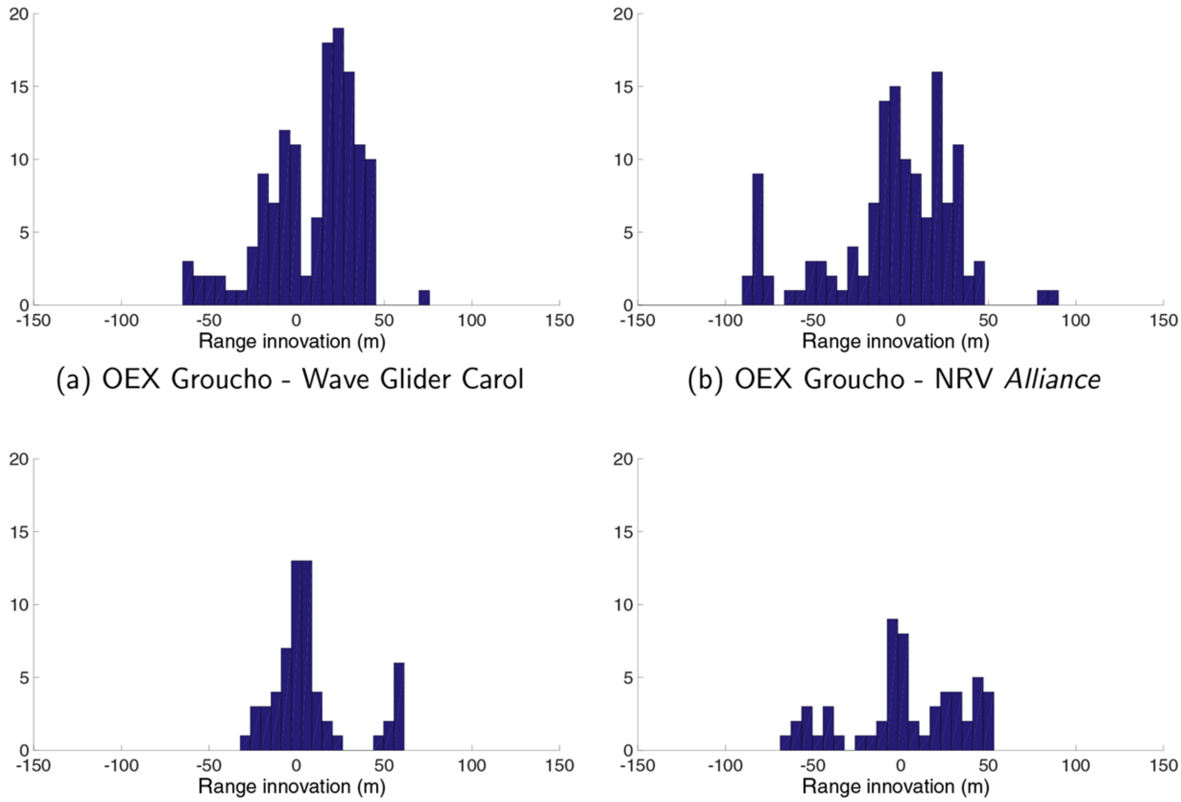

(a) OEX Groucho - Wave Glider Carol

(b) OEX Groucho - NRV *Alliance*

(c) OEX Groucho - Gateway

(d) OEX Groucho - Wave Glider Lisa

Figure 18. Distribution of the range measurement error between OEX Groucho and the nodes of the network. The distributions show that the range measurements are not zero mean and not Gaussian distributed.

while experiencing prolonged periods of no communications, the maximum navigation error was about 350 m and the filter was still able to recover reducing the error as soon as new measurements became available.

6. CONCLUSION AND FUTURE DEVELOPMENT

This paper described an acoustic network–based system to support underwater navigation of AUVs. The approach is based on the addition of localization services to networked acoustic communications. Traditional approaches to AUV navigation, such as LBL and/or USBL methods, require the AUVs to query one or more modems/transponders while measuring the two-way travel time of the acoustic packets. Although these methods have been integrated together with communications devices, this has been usually done at the level of the acoustic modem. In this respect, the approach proposed herein is more generic: The localization data are synthesized directly with regular communication traffic and is designed to be applicable to generic, including software-defined, modems.

The proposed acoustic network navigation system has been deployed for the first time in real time during the COLLAB-NGAS14 sea trial, held in October 2014, off the coast of West Italy. The underwater network was composed of four fixed nodes, and two CMRE OEX AUVs, and it was able to provide localization services for the vehicles supporting their navigation during the entire mission. The navigational service, implemented at application level, was able to exploit the availability of the modems' transmission and reception time stamps, and to use this information to calculate the associated packet propagation time, while not relying on specific modem features (e.g., physical-level acknowledgments) or dedicated hardware (e.g., synchronized clocks). These data together with the sound speed and the corresponding position of the remote node made it possible to obtain a range measurement from the remote node itself, which hence could be used within the vehicle's navigation filter. The described acoustic network navigation system is general: It does not add any design constraints to the network; it only uses a minimal and well defined interface with the rest of the system, and it only requires a limited amount of additional bandwidth. To the best of our knowledge, this was the first time that such a system was demonstrated at sea. Results have shown how the proposed network-based interrogation scheme is effective in limiting the navigation error, even at long ranges and with sporadic communication.

In the deployed system, specific implementation choices have been based on time-triggered transmissions as made available from the acoustic modems. This does not limit the applicability of the approach to other types of modems, but indeed made the implementation simpler. In general, however, this is not necessary and the same scheme can be applied using normal transmissions, as long as the necessary bookkeeping is done at network/application level. Several improvements can be foreseen for the system. First, the inclusion of Doppler measurements, as calculated by the acoustic modems when decoding an acoustic packet, can be effective in refining the range measurements. The delay between an interrogation and its reply depends on how reactive the MAC is in allowing a short TAT. Future work will compare how different MAC layers can have different impact on the resulting ranging performance.

Several sources of errors concurrently affect the overall localization performance of the system, and the impact of each component is difficult to isolate. At the same time, having a careful characterization of the errors is certainly a necessary requirement to understand the limits of the proposed approach. This, however, requires a dedicated investigation and specific experimental activities, possibly in controlled environments, and goes outside the scope of this work. Future studies will try to tackle these specific issues.

The choice of the EKF as a navigation filter for the vehicles was driven by its implementation simplicity, reduced computational load when compared with alternative approaches that do not require linearization or assumption on noise statistics (e.g., particle filters), and by its wide usage as a tool for navigation in today's AUVs. In this work, this proved to be enough to demonstrate, in the field, the effectiveness of the acoustic network navigation system. However, the analysis of the experimental data has shown that some of the assumptions of the EKF are not fully respected. For instance, measurement errors are not zero mean or white. Furthermore, in more dramatic conditions with respect to those encountered in this work (e.g., longer ranges and more network nodes), the error induced by the relative motion of the vehicles may impact on the filter linearization points. New CPUs that have been recently installed on the CMRE OEXs will make possible, in the future, to investigate the usage of alternative nonparametric navigation filters that are able to take into account non-Gaussian measurement errors and the nonlinearity of the measurements. Moreover, means to compensate for node relative motion by tracking the position of the network nodes, especially during periods of no communications, with dedicated real-time filters will be investigated.

Finally, it is worth pointing out that the same information can be used to include more services into the network. In particular, transmission and reception time stamp exchange can also be used to calculate the relative clock offset and drift between any two nodes in the network, and hence to clock-synchronize the nodes. The availability of a network timing service, similar to the network time protocol (NTP) available in terrestrial networks, will open new scenarios, as for instance, the possibility to have a network-enabled OWTT navigation.

ACKNOWLEDGMENTS

This work has been supported by the NATO Allied Command Transformation (ACT), under the Collaborative Anti-Submarine Warfare Programme, projects "System Concepts for Littoral Surveillance" (Project 1) and "Communications and Networks in the Maritime Environment" (Project 2), and by the Office of Naval Research Global under grant no. N62909-16-1-2095.

The authors would like to thank everyone involved in the COLLAB–NGAS14 sea trial, including Kevin LePage and Ryan Goldhahn (scientists in charge), Vittorio Grandi (engineering coordinator), everyone in the Engineering Department, and the captain and the crew of the NRV *Alliance*. This work also owes a great deal to Joao Alves (Project 2 leader), Arjan Vermeij, Bruno Cardeira, and Tom Furfaro. Their insights and suggestions have made this work possible.

REFERENCES

Akyildiz, I. F., Pompili, D., & Melodia, T. (2005). Underwater acoustic sensor networks: Research challenges. Ad Hoc Networks, 3(3), 257–279.

Allotta, B., Bartolini, F., Caiti, A., Costanzi, R., Corato, F. D., Fenucci, D., Gelli, J., Guerrini, P., Monni, N., Munafò, A., Natalini, M., Pugi, L., Ridolfi, A., & Potter, J. (2015). Typhoon at CommsNet13: Experimental experience on auv navigation and localization. Annual Reviews in Control, 40, 157–171.

Allotta, B., Caiti, A., Costanzi, R., Fanelli, F., Fenucci, D., Meli, E., & Ridolfi, A. (2016). A new AUV navigation system exploiting unscented Kalman filter. Ocean Engineering, 113, 121–132.

Alves, J., Potter, J., Guerrini, P., Zappa, G., & Lepage, K. (2014). The LOON in 2014: Test bed description," 2014 Underwater Communications and Networking (UComms), Sestri Levante, 1–4.

Anjangi, P., & Chitre, M. (2016). Unslotted transmission schedules for practical underwater acoustic multihop grid networks with large propagation delays, Paper Presented at Proceedings of the Underwater Communication Conference (UComms).

Arambel, P. O., Rago, C., & Mehra, R. K. (2001). Covariance intersection algorithm for distributed spacecraft state estimation, Paper Presented at Proceedings of the American Control Conference.

Bahr, A., Leonard, J. J., & Fallon, M. F. (2009a). The International Journal of Robotics Research, 28(6), 714–728.

Bahr, A., Walter, M. R., & Leonard, J. J. (2009b). Consistent cooperative localization, 2009 IEEE International Conference on Robotics and Automation, Kobe, Japan (pp. 3415–3422).

Benjamin, M. R. (2002). Interval programming: A multi-objective optimisation model for autonomous vehicle control. Unpublished PhD thesis, Beown University, Providence, RI.

Benjamin, M. R., Newman, P. M., Leonard, J. J., Newman, P., & Schmidt, H. (2009). Extending a MOOS-IvP autonomy system and users guide to the IvPBuild toolbox. Technical report, Massachusetts Institute of Technology and Woods Hole Oceanographic Institution.

Benjamin, M. R., Schmidt, H., Newman, P. M., & Leonard, J. J. (2010). Nested autonomy for unmanned marine vehicles with MOOS-IVP. Journal of Field Robotics, 27(6), 834–875.

Caiti, A., Calabrò, V., Fabbri, T., Fenucci, D., & Munafò, A. (2013a). Underwater communication and distributed localization of AUV teams. In 2013 MTS/IEEE OCEANS - Bergen, Bergen, 1–8.

Caiti, A., Calabro, V., Fusini, L., Munafò, A., Grythe, K., Hovem, J., Lie, A., & Reinen, T. (2012a). Underwater acoustic network performance: Results from the UAN11 sea trial. Paper Presented at *Oceans, 2012* (pp. 1–8).

Caiti, A., Calabrò, V., & Munafò, A. (2012b). AUV team cooperation: emerging behaviours and networking modalities. IFAC Proceedings Volumes, 45(27), 342–347.

Caiti, A., Grythe, K., Hovem, J. M., Jesus, S. M., Lie, A., Munafò, A., Reinen, T. A., Silva, A., & Zabel, F. (2013b). IEEE Journal of Oceanic Engineering, 38(4), 758–771.

Canepa, G., Munafò, A., Murphy, S., Micheli, M., & Morlando, L. (2015). Paper Presented at IEEE/MTS Conf. OCEANS15.

Casalino, G., Caiti, A., Simetti, E., & Turetta, A. (2011). Rt2: Real time ray tracing for underwater range evaluation. Intelligent Service Robotics, 4(4), 259–270.

Chitre, M., Bhatnagar, R., & Soh, W.-S. (2014). Unetstack: An agent-based software stack and simulator for underwater networks, Paper Presented at Oceans - St. John's, 2014 (pp. 1–10).

Evologics GmbH. (2015). S2cr 7/17 acoustic modem.

Fallon, M. F., Papadopoulos, G., Leonard, J. J., & Patrikalakis, N. M. (2010). Cooperative AUV navigation using a single maneuvering surface craft. The International Journal of Robotics Research, 29(12), 1461–1474.

Ferri, G., Manzi, A., Fornai, F., Ciuchi, F., & Laschi, C. (2015). The hydronet asv, a small-sized autonomous catamaran for real-time monitoring of water quality: From design to missions at sea. IEEE Journal of Oceanic Engineering, 40(3), 710–726.

Ferri, G., Munafò, A., Goldhahn, R., & LePage, K. (2014). A non-myopic, receding horizon control strategy for an AUV to track an underwater target in a bistatic sonar scenario, 53rd IEEE Conference on Decision and Control, Los Angeles, CA, 5352–5358.

Fossen, T. I. (2011). Handbook of marine craft hydrodynamics and motion control. Hoboken, NJ: Wiley.

Freitag, L., Grund, M., Partsan, J., Singh, S., Koshi, P., & Ball, K. (2005). The WHOI Micro-Modem: an acoustic communication and navigation system for multiple platforms, Paper Presented at Proceedings of IEEE/MTS Oceans 2005.

Freitag, L., Johnson, M., Grund, M., Singh, S., & Preisig, J. (2001). Integrated acoustic communication and navigation for multiple UUVs, Paper Presented at Proceedings of IEEE/MTS Conference on Oceans, Honolulu, HI.

Furfaro, T. C., & Alves, J. (2014). An application of distributed long baseline short-range node localisation in an underwater network. Paper Presented at UComms (pp. 1–5).

Hiller, T., Steingrimsson, A., & Melvin, R. (2012). Positioning small AUVs for deeper water surveys using inverted USBL, Paper Presented at Hydro12 - Taking Care of the Sea.

Hunt, M. M., Marquet, W. M., Moller, D. A., Peal, K. R., Smith, W. K., & Spindel, R. C. (1974). An acoustic navigation system, Technical report, Woods Hole Oceanographic Institution.

Kebkal, K. G., Kebkal, O. G., Kebkal, V. K., & Petroccia, R. (2014). Synchronization tools of acoustic communication devices in control of underwater sensors, distributed antennas, and autonomous underwater vehicles. Gyroscopy and Navigation, 5(4), 257–265.

Kebkal, O., Kebkal, K., & Bannasch, R. (2011). Long-baseline hydro-acoustic positioning using D-MAC communication protocol. Paper Presented at Proceedings of IEEE OCEANS 2012.

Kongsberg, Maritime. (2015). Acoustic underwater positioning and navigation systems hipap.

Liquid Robotics. (2015). Wave gliders v2.

Milne, P. H. (1983). Underwater acoustic positioning systems. Spon, London.

Munafò, A., Sliwka, J., Ferri, G., Vermeij, A., Goldhahn, R., LePage, K., Alves, J., & Potter, J. (2014). Enhancing AUV localisation using underwater acoustic sensor networks: results in long-base line navigation from the COLLAB13 sea trial. Paper Presented at Proceedings of IEEE/MTS Oceans 2014, St. John's.

Paull, L., Saeedi, S., Seto, M., & Li, H. (2014a). AUV navigation and localization: A review. IEEE Journal of Oceanic Engineering, 39(1), 131–149.

Paull, L., Seto, M., & Leonard, J. J. (2014b). Decentralized cooperative trajectory estimation for autonomous underwater vehicles, 2014 IEEE/RSJ International Conference on Intelligent Robots and Systems, Chicago, IL, pp. 184–191. doi: 10.1109/IROS.2014.6942559

Petroccia, R., Petrioli, C., & Sotjanovi, M. (2008). A comparative performance evaluation of mac protocols for underwater sensor networks, Paper Presented at Proceedings of the IEEE/MTS OCEANS Conference.

Pompili, D., & Akyildiz, I. F. (2010). A multimedia cross-layer protocol for underwater acoustic sensor networks. IEEE Transactions on Wireless Communications, 9(9), 2924–2933.

Potter J. et al. (2014). Software Defined Open Architecture Modem development at CMRE, 2014 Underwater Communications and Networking (UComms), Sestri Levante, pp. 1–4. doi: 10.1109/UComms.2014.7017157, URL: http://ieeexplore.ieee.org/stamp/stamp.jsp?tp=&arnumber=7017157&isnumber=7017115

Rice, J. A. (2002). Undersea networked acoustic communication and navigation for autonomous mine-countermeasure systems. Paper Presented at International Symposium on Technology and the Mine Problem.

Rice, J. A. (2005). Seaweb acoustic communication and navigation networks. Paper Presented at International Conference on Underwater Acoustic Measurements: Technologies and Results, Heraklion, Crete, Greece.

Schneider, T., & Schmidt, H. (2010). The dynamic compact control language: A compact marshalling scheme for acoustic communications. Paper Presented at IEEE OCEANS Conference.

Schneider, T. E. (2013). Advances in integrating autonomy with acoustic communications for intelligent networks of marine robots. Unpublished Ph.D. thesis, Massachusetts Institute of Technology and Woods Hole Oceanographic Institution.

Singh, S., Grund, M., Bingham, B., Eustice, R., Singh, H., & Freitag, L. (2006). Underwater Navigation with the WHOI Micro-Modem. Paper Presented at Proc. of IEEE/MTS Oceans 2006.

Vaganay, J., Leonard, J., Curcio, J., & Willcox, J. (2004). Experimental validation of the moving long base-line navigation concept. In IEEE/OES Autonomous Underwater Vehicles, 2004 (pp. 59–65).

Vermeij, A., & Munafò, A. (2015). A Robust, Opportunistic Clock Synchronization Algorithm for Ad Hoc Underwater Acoustic Networks. In IEEE Journal of Oceanic Engineering, 40(4), 841–852.

Vickery, K. (1998). Acoustic positioning systems. A practical overview of current systems, Proceedings of the 1998 Workshop on Autonomous Underwater Vehicles (Cat. No. 98CH36290), Cambridge, MA, pp. 5–17.

Walls, J. M., Cunningham, A. G., & Eustice, R. M. (2015). Cooperative localization by factor composition over a faulty low-bandwidth communication channel, 2015 IEEE International Conference on Robotics and Automation (ICRA), Seattle, WA, pp. 401–408. doi: 10.1109/ICRA.2015.7139030, URL: http://ieeexplore.ieee.org/stamp/stamp.jsp?tp=&arnumber=7139030&isnumber=7138973.

Walls, J. M., & Eustice, R. M. (2011). Experimental comparison of synchronous-clock cooperative acoustic navigation algorithms. Paper presented a IEEE OCEANS 2011.

Webster, S. E., Eustice, R. M., Singh, H., & Whitcomb, L. L. (2012). Advances in single-beacon one-way-travel-time acoustic navigation for underwater vehicles. The International Journal of Robotics Research, 31(8), 935–950.